ORIGINAL PAPER

Nile Blue and Indigo Carmine organic dyes as corrosion inhibitor of mild steel in hydrochloric acid

Madjid Abdeli · Naghi Parvini Ahmadi ·
Rasoul Azari Khosroshahi

Abstract The inhibiting behavior of Nile Blue and Indigo Carmine organic dyes on mild steel corrosion was evaluated in 1 M HCl solution, separately, by weight loss, potentiodynamic polarization, and electrochemical impedance spectroscopy techniques. Results show that the inhibition efficiency (%IE) increases with the increasing concentration of Indigo Carmine up to 9.65×10^{-05} M (%IE~98) and Nile Blue up to 1.08×10^{-04} (%IE~75–80). Good agreement was found between the results obtained from the different techniques used. Polarization curves indicate that the inhibition of the both inhibitors is of a mixed anodic–cathodic nature, and Langmuir isotherm is found to be an accurate isotherm describing the adsorption behavior. The inhibition mechanism of the inhibitors involves chemisorption interaction between the inhibitor and the mild steel. The inhibition efficiency for both inhibitors decreased by the rising temperature in the range of 25–55°C, and these results verified the chemisorption behavior of both the inhibitors.

Keywords Inhibitor · Organic dye · Indigo Carmine · Nile Blue

Introduction

Hydrochloric acid is generally used in industry as chemical cleaning, oil well cleaning, descaling, and pickling for the removal of undesirable scale and rust from the metallic surfaces. The corrosion of steel is an important concern that has received a considerable amount of attention [1–5]. Using inhibitors is an important method of protecting materials against acid attack, reducing the metal dissolution and the consumption of acid. Most of the effective corrosion inhibitors are organic compounds containing nitrogen, sulfur, and oxygen atoms. The efficiency of an organic compound as an inhibitor is mainly dependent on its ability to get adsorbed on metal. These inhibitors contain oxygen, nitrogen, sulfur heteroatoms, and multiple bonds. This phenomenon is influenced by the nature and surface charge of the metallic surface, testing media, and chemical structure of inhibitors [6–10]. Investigating and exploring new corrosion inhibitor for steel corrosion in acid solutions are important for its practical application. Recently, several researches [11–19] have reported on the investigation of organic dyes as corrosion inhibitors, and their attempts have been made to highlight the efficacy of some organic dyes as potential inhibitors of metal corrosion in acidic media, and the use of organic dyes as a new class of inhibitors with low toxicity and good efficiency has been rarely cited.

In this work, the corrosion inhibition of Nile Blue (($C_{20}H_{20}N_3O)HSO_4$) and Indigo Carmine ($C_{16}H_8N_2Na_2O_8S_2$) organic dyes on mild steel in 1 M HCl have been studied separately by using weight loss method, potentiodynamic polarization, and electrochemical impedance spectroscopy (EIS) techniques. The selected organic dyes containing nitrogen and oxygen atoms and some multiple bonds with relatively high molecular weight belong to color components. This study is helpful in efforts to develop new inhibitors with good efficiency and also to further explain the mechanisms of the inhibition process.

M. Abdeli · N. P. Ahmadi (✉) · R. A. Khosroshahi
Material Faculty of Sahand University of Technology,
Tabriz, Iran
e-mail: parvini@sut.ac.ir

Experimental details

Materials

Mild steel specimens with the chemical composition shown in Table 1 were used to perform the experiments. The specimens were ground with different emery papers (grade 400, 600, 800, 1,000, and 1,200), rinsed with distilled water, degreased in absolute ethanol, and then dried. The molecular structure of Indigo Carmine and Nile Blue are given in Figs. 1 and 2. The employed concentration range of Indigo Carmine and Nile Blue were from 2.14×10^{-06} to 12.9×10^{-05} and 2.41×10^{-06} to 1.08×10^{-04} mol/l, respectively. The aggressive solution (1 M HCl) is prepared by dilution of analytical grade 37% HCl with double distilled water. In all experiments, the volume of test solutions for each experiment was 200 ml, and the temperature of the solutions was controlled by thermostat.
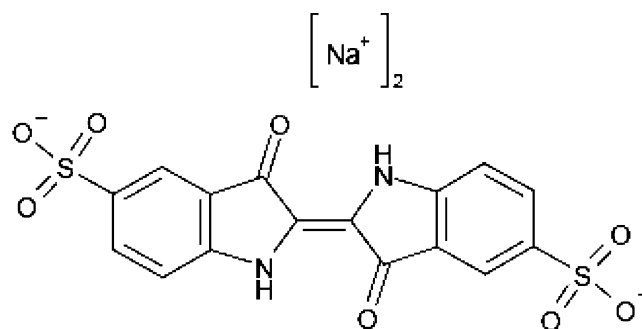
Electrochemical measurements

Polarization and EIS experiments were carried out using a potentiostat/galvanostat (EG&G model 273A), frequency response analyser (Solarton model SI 1255), respectively. For electrochemical measurements, a conventional electrochemical Pyrex glass cell was used containing three compartments for working, platinum counter, and a saturated calomel electrode (SCE) as reference. The working mild steel electrode was embedded in Araldite to offer its cross-sectional area (1 cm^2) in contact with the solution. The steady-state open-circuit potential (OCP) was noted at the end of 60 min, then the Tafel polarization scan was carried out by polarizing to ±250 mV with respect to the OCP at a scan rate of 1 mV s^{-1} from the cathodic side. In polarization method, Stern–Geary equation [20] (Eq. 1) and Eq. 2 were used to calculate corrosion current ($i_{Corr.}$) and the inhibition efficiency (%IE), respectively, where I_{Corr} and $I_{Corr(inh)}$ are the corrosion current density values of the steel electrode in 1 M HCl solutions without and with the inhibitor, respectively.

$$i_{Corr.} = \frac{b_a \times b_c}{2.303 \times R_p (b_c + b_a)} \tag{1}$$

$$\%IE = \frac{I_{Corr} - I_{Corr(inh)}}{I_{corr}} \times 100 \tag{2}$$

Fig. 1 Chemical structure of Indigo Carmine

The polarization resistance (R_p) was calculated at overvoltage lower than ±20 mV. Tafel slopes were calculated at over voltage more than ±70 mV in the Tafel regions. EIS measurements were carried out in a frequency range of 100 kHz to 10 mHz using an amplitude of 5 mV peak to peak using A.C. signal at the open circuit potential, and in this method, %IE was calculated by using Eq. 3:

$$\%IE = \frac{R_{ct(inh)} - R_{ct}}{R_{ct(inh)}} \times 100 \tag{3}$$

Where R_{ct} and $R_{ct(inh)}$ are the charge-transfer resistances of mild steel in blank and inhibited solution.

Weight loss measurements

The used steel specimens had a rectangular form (length =2 cm, width =1.5 cm, thickness =1 cm).

The samples were carefully weighted and immersed in non-stirring test solutions for 24 h, and at the end, the specimens were washed in acetone, dried, and then weighed. Inhibition efficiency was determined using Eq. 4, where $W_{Corr(inh)}$ and W_{Corr} are the corrosion rates of mild steel with and without the inhibitor, respectively.

$$\%IE = \frac{w_{corr} - w_{corr(inh)}}{R_o} \times 100 \tag{4}$$

Results and discussion

Polarization studies

Figures 3 and 4 show the influence of Indigo Carmine and Nile Blue concentration on the cathodic and anodic
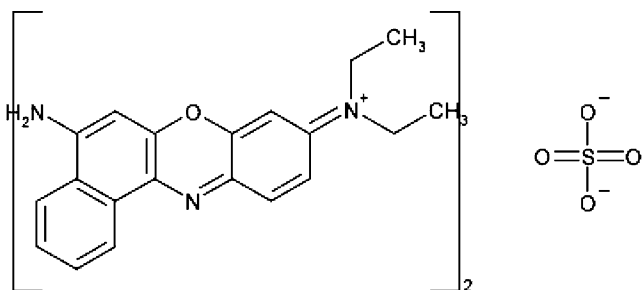
Table 1 Chemical composition of mild steel sample

Element	C	Si	Mn	P	S	Cr	Mo	Co	Fe
wt.%	0.18	<0.050	0.366	0.0279	0.0079	0.0051	0.0146	0.0307	Balance

Fig. 2 Chemical structure of Nile Blue

Fig. 4 Potentiodynamic polarization curves for the mild steel electrode in 1 M HCl solutions containing different concentrations of Nile Blue at 25°C

polarization curves of steel in 1 M HCl at 25°C, respectively. Related electrochemical corrosion parameters and calculated inhibition efficiency of each inhibitor are collected in Table 2. As shown in Figs. 3 and 4, increasing the Indigo Carmine and Nile Blue concentration reduces both the related cathodic and the anodic currents. Theses inhibitors are considered as a mixed-type inhibitor because the cathodic and anodic current densities decrease upon introducing the inhibitor in the aggressive solution. So the addition of the Indigo Carmine and Nile Blue reduces the anodic dissolution and also retards the cathodic hydrogen evolution reaction. The inhibition efficiency of Indigo Carmine increases with C_{inh} reaching its maximum value, 98.76%, at 9.65×10^{-05} M. Above this concentration, the %IE slightly decreases. Like Indigo Carmine, the inhibition efficiency of Nile Blue increases with C_{inh} reaching its maximum value, 75.42%, at 1.08×10^{-04} M, but above this concentration, the solubility of Nile Blue decreases and it started to precipitate.

EIS studies

Nyquist plots for mild steel in 1 M HCl solution in the absence and presence of inhibitor at various concentrations of the studied inhibitors (at 25°C) are shown in Figs. 5 and 6. The semicircle Nyquist plots can be modeled by a simple "Randles" circuit, including the "charge-transfer resistance" (R_{ct}) parallel with double layer capacitance (C_{dl}) in series with solution resistance (R_s). As shown in Figs. 5 and 6, the Nyquist plots for mild steel in 1 M HCl for the both inhibitors were not perfect semicircles. This difference can be explained by the non-ideal behavior of double layer as a capacitor. Therefore it is necessary to use a constant phase element (CPE) instead of double layer capacity to account for non-ideal behavior. The appearance of the CPE element is often related to the electrode roughness or to the inhomogeneity in the conductance or dielectric constant [20,21]. The CPE can be modeled as follows [22]:

$$Z_{CPE} = (j\omega C)^{-\alpha} \qquad (5)$$

Where Z_{CPE} is the impedance, j is the square root of -1, ω is the frequency, C is the capacitance, and α is a measure of the non-ideality of the capacitor and has a value in the range of $0 < \alpha < 1$. The quantitative results of impedance measurements (calculated by Zview program) for the Indigo Carmine and Nile Blue are given in Table 3. Inspection of the data in Fig. 5 and Table 3 for the Indigo Carmine reveals that the corrosion of mild steel was decreased in the presence of the inhibitor because the charge-transfer resistance of mild steel was significantly increased. As shown in Fig. 6 and Table 3, the same results were obtained for the Nile blue. It is apparent from the figures that the charge-transfer resistance value of mild
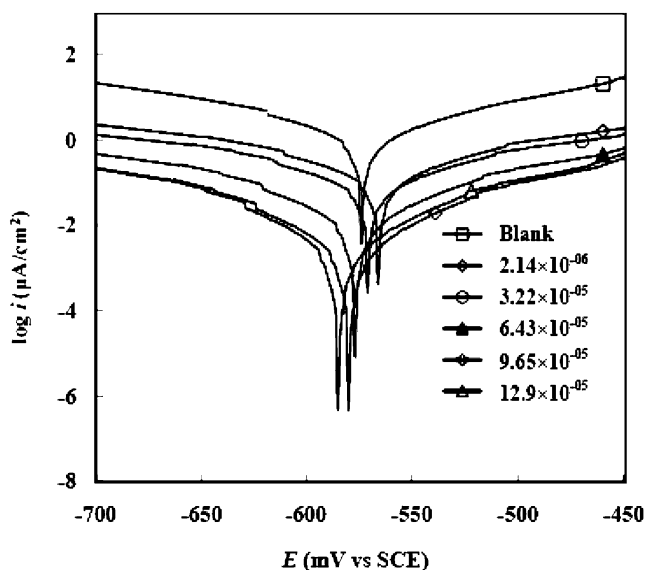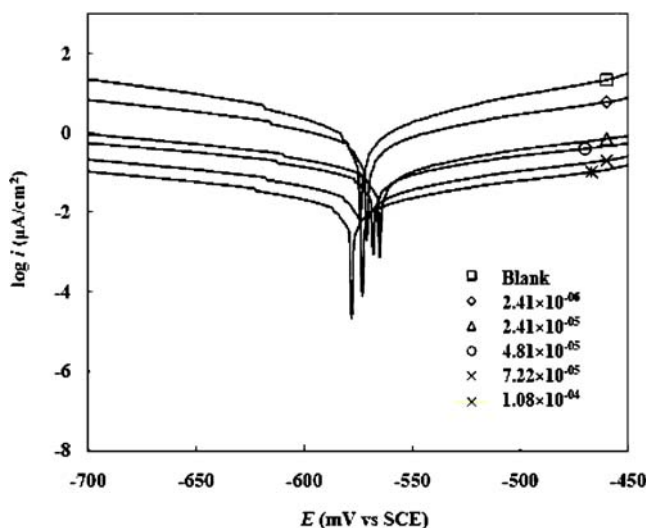

Fig. 3 Potentiodynamic polarization curves for the mild steel electrode in 1 M HCl solutions containing different concentrations of Indigo Carmine at 25°C
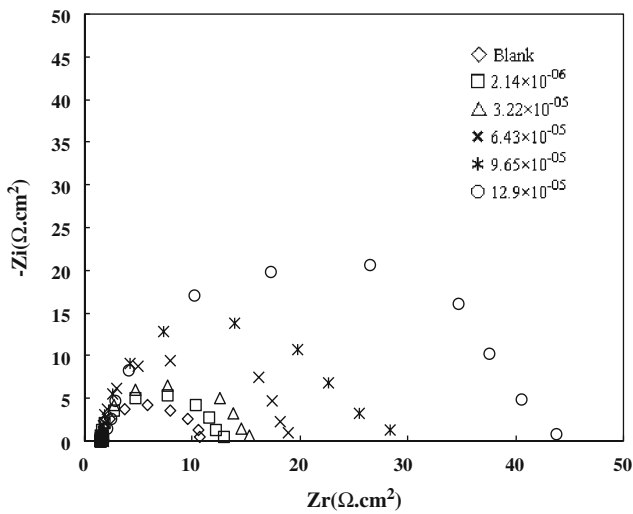
Table 2 Polarization parameters for mild steel in 1 M hydrochloric acid in the absence and presence of Indigo Carmine and Nile Blue at various concentrations (at 25°C)

Concentration (M)	b_a (mV/dec)	$-b_C$ (mV/dec)	R_p (Ωcm^2)	$i_{Corr.}$ (mA/cm^2)	$E_{corr.}$ (mV (vs SCE))	%IE
Indigo Carmine						
Blank	84	135	12.57	1.79	−574	–
2.14×10^{-06}	68	124	22.27	0.85	−566	52.43
3.22×10^{-05}	64	123	29.14	0.63	−571	64.75
6.43×10^{-05}	63	119	61.25	0.29	−577	83.68
9.65×10^{-05}	57	117	844.13	0.02	−580	98.76
12.9×10^{-05}	56	115	421.57	0.04	−585	97.53
Nile Blue						
Blank	84	135	12.57	1.79	−574	–
2.41×10^{-06}	81	129	14.83	1.45	−571	18.99
2.41×10^{-05}	78	127	16.61	1.26	−565	29.61
4.81×10^{-05}	75	122	19.82	1.02	−568	43.017
7.22×10^{-05}	71	118	28.52	0.68	−573	62.011
1.08×10^{-04}	67	112	41.52	0.44	−578	75.42

steel in uninhibited HCl solution significantly changes after the addition of the inhibitors. For both inhibitors, increasing their concentrations increases R_{ct} and decreases the value of CPE and consequently enhances %IE till reaching their maximum values at 9.65×10^{-05}M (R_{ct}=833.75, %IE=98.71) for the Indigo Carmine and at 1.08×10^{-04}M (R_{ct}=43.86, %IE= 80.41) for the Nile Blue. Increase of charge-transfer resistance

with inhibitor concentration may be a result of more inhibitor molecule adsorption on the metal surface at higher concentration of the inhibitors. Decrease of CPE may be caused by a reduction in local dielectric constant and/or by an increase in the thickness of the electrical double layer. These results suggest that the inhibitor molecules act by adsorption at the metal/solution interface [1,11].

Fig. 5 Nyquist diagrams for the mild steel electrode in 1 M HCl solutions in the absence and presence of Indigo Carmine at various concentrations at 25°C
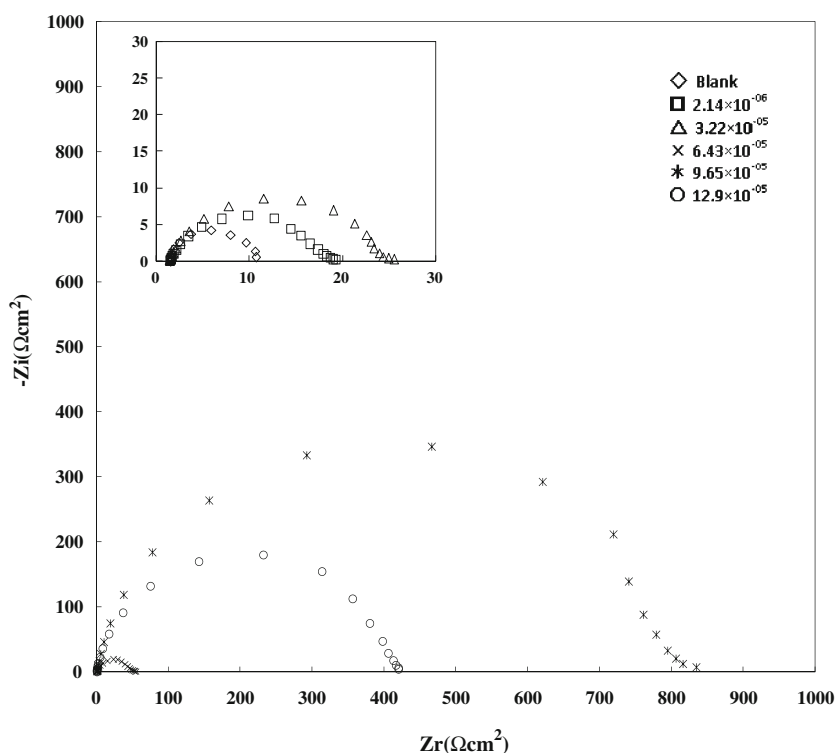
Fig. 6 Nyquist diagrams for the mild steel electrode in 1 M HCl solutions in the absence and presence of Nile Blue at various concentrations at 25 °C

Table 4 Weight loss results for mild steel in 1 M hydrochloric acid in the absence and presence of Indigo Carmine and Nile Blue at various concentrations (at 25 °C)

Concentration (M)	Rate (g/cm²h)	%IE
Indigo Carmine		
Blank	3.81×10^{-03}	–
2.14×10^{-06}	2.04×10^{-03}	46.58
3.22×10^{-05}	1.55×10^{-03}	59.45
6.43×10^{-05}	8.83×10^{-04}	76.86
9.65×10^{-05}	7.17×10^{-05}	98.12
12.9×10^{-05}	1.37×10^{-04}	96.42
Nile Blue		
2.41×10^{-06}	3.04×10^{-03}	20.23
2.41×10^{-05}	2.61×10^{-03}	31.67
4.81×10^{-05}	2.07×10^{-03}	45.68
7.22×10^{-05}	1.30×10^{-03}	65.79
1.08×10^{-04}	8.69×10^{-04}	77.21

Weight loss studies

Table 4 shows weight loss results for mild steel in 1 M HCl in the absence and presence of Indigo Carmine at various concentrations (at 25 °C), as shown by the inhibition efficiency increase with increasing inhibitor concentration and reaches to its maximum value at 9.65×10^{-05} M (%IE= 98.12). Table 4 also shows the weight loss results of Nile

Table 3 Electrochemical impedance measurement of mild steel in 1 M hydrochloric acid in the absence and presence of Indigo Carmine and Nile Blue at various concentrations (at 25 °C)
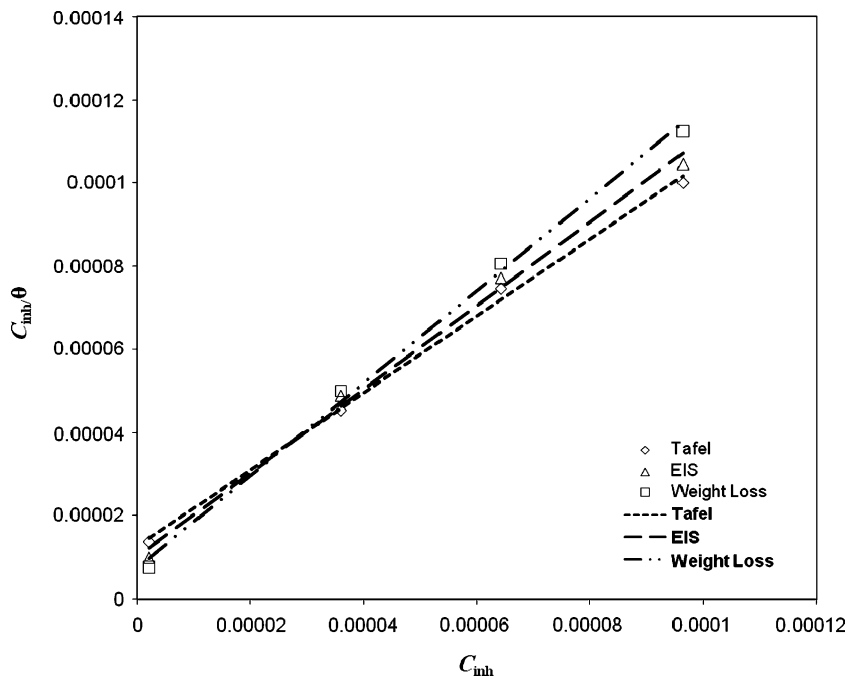
Concentration (M)	R_S (Ωcm²)	CPE (Fcm⁻²)	α	R_{CT} (Ωcm²)	%IE
Indigo Carmine					
Blank	1.56	2.60×10^{-04}	0.99	10.78	–
% error	1.2	4.9	0.9	1.4	
2.14×10^{-06}	1.53	3.90×10^{-05}	0.91	19.35	44.29
% error	1.1	3.4	0.5	0.8	
3.22×10^{-05}	1.45	3.25×10^{-05}	0.87	25.55	57.81
% error	0.4	1.9	0.3	0.3	
6.43×10^{-05}	1.51	2.70×10^{-05}	0.84	56.22	80.97
% error	1.8	4.9	0.9	1.2	
9.65×10^{-05}	1.36	6.86×10^{-06}	0.81	833.75	98.71
% error	1.2	1.1	0.14	0.33	
12.9×10^{-05}	1.1	1.36×10^{-05}	0.81	420.85	97.44
% error	0.7	0.8	0.09	0.2	
Nile Blue					
Blank	1.56	2.60×10^{-04}	0.99	10.78	–
% error	1.2	4.9	0.9	1.4	
2.41×10^{-06}	1.57	4.46×10^{-05}	0.89	13.31	23.74
% error	1.3	3.5	0.9	1.9	
2.41×10^{-05}	1.61	4.10×10^{-05}	0.85	15.32	34.85
% error	1.2	4.6	0.8	2.2	
4.81×10^{-05}	1.73	3.38×10^{-05}	0.85	18.92	48.54
% error	1.2	3.9	0.9	1.8	
7.22×10^{-05}	1.82	2.11×10^{-05}	0.80	28.37	69.52
% error	1.3	4.2	0.9	1.8	
1.08×10^{-04}	1.95	1.85×10^{-05}	0.79	43.86	80.41
% error	1.2	4.1	0.8	2.4	

Fig. 7 Langmuir adsorption plot of various used techniques for mild steel in 1 M HCl containing different concentration of Indigo Carmine at 25 °C


Blue and also is shown that the maximum efficiency was obtained at 8.69×10^{-04} M (%IE=77.21).

Adsorption isotherms

Organic corrosion inhibitors decrease metal dissolution via adsorption on the metal/corrodent interface to form a protective film, which separates the metal surface from the corrosive medium. The adsorption route is usually regarded as a substitution process between the organic inhibitor in the aqueous solution and water molecules adsorbed at the metal surface [10]. The adsorption isotherm can give information on the metal–inhibitor interaction. Considering the inhibitor efficiencies at various concentrations of both inhibitors, obtained by various used techniques, it revealed that the surface coverage values, θ, (θ=%IE/100), increased with the increasing concentration of the inhibitor. Supposing that molecular adsorption at the

Fig. 8 Langmuir adsorption plot of various used techniques for mild steel in 1 M HCl containing different concentration of Nile Blue at 25 °C
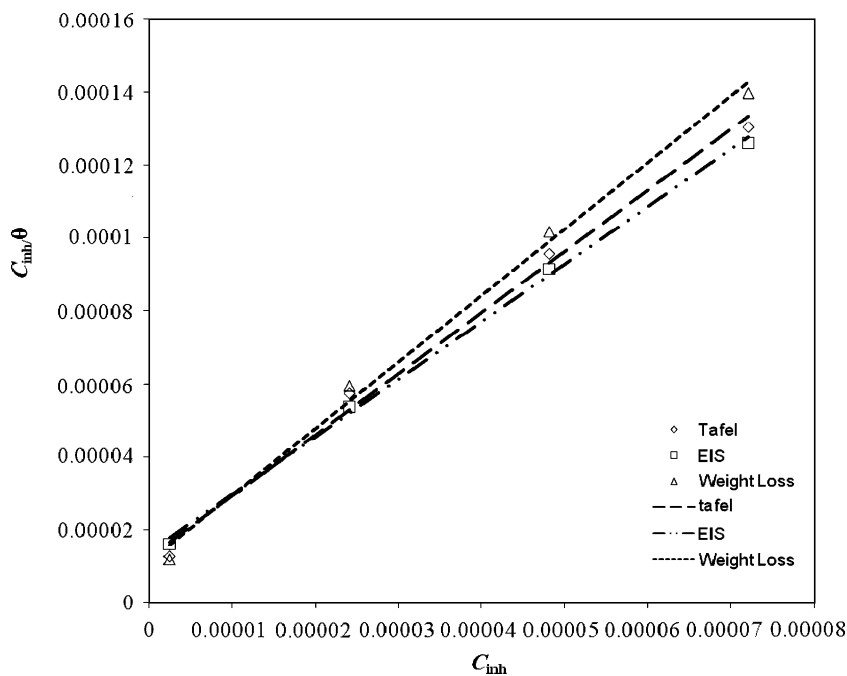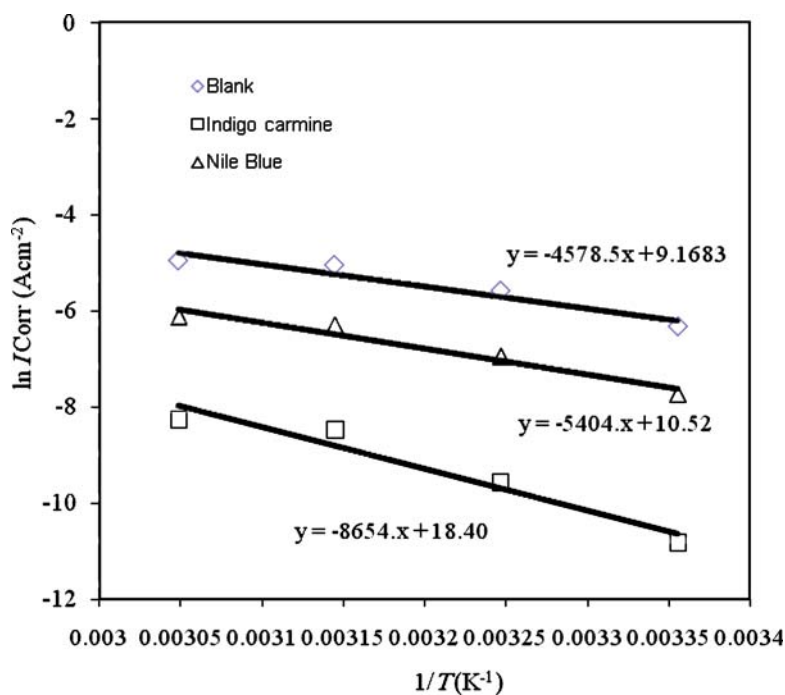
Table 5 The values of binding constant (K) and free energy of adsorption (ΔG_{ads}) calculated using different methods for the Indigo Carmine and Nile Blue at 25°C

Method	Weight loss	Polarization	EIS
Indigo Carmine			
K	104,500	78,000	81,000
ΔG_{ads} (kJ/mol)	−38.56	−37.84	−37.93
Nile Blue			
K	74,600	98,000	73,500
ΔG_{ads} (kJ/mol)	−35.5	−35.2	−35.8

Table 6 Effect of temperature on the inhibition efficiency of Indigo Carmine (9.65×10^{-05} M) and Nile Blue (1.08×10^{-04} M) in 1 M hydrochloric acid without (I_{Corr}) and with ($I_{Corr(inh)}$) the inhibitors

T (°C)	I_{Corr} (mA/cm^2)	$I_{Corr(inh)}$ (mA/cm^2)	%IE
Indigo Carmine			
25	1.79	0.02	98.76
35	3.76	0.07	98.12
45	6.41	0.21	96.86
55	7.05	0.26	96.24
Nile Blue			
25	1.79	0.44	75.42
35	3.76	0.97	74.12
45	6.41	1.86	70.85
55	7.05	2.21	68.76

metal/solution interface is the mechanism through which the corrosion inhibition occurs, several adsorption isotherms can be tested. To describe Indigo Carmine and Nile Blue adsorption behaviors, various adsorption isotherms [9,11,22] were used, and the Langmuir kinetic–thermodynamic model fits the experimental data well for the both inhibitors. Figures 7 and 8 show the Langmuir adsorption plot of various techniques used for mild steel in 1 M HCl containing a different concentration of both the inhibitors at 25°C, and a similar behavior was observed at other temperatures (35, 45, and 55°C). The Langmuir isotherm assumes that the molecules adsorbed from the monolayer, and there are no interactions between the adsorbed molecules [20]. By using the Langmuir adsorption isotherm, K values (the equilibrium constant of the process of adsorption) and free energy of adsorption (by using Eq. 6) of the three methods were calculated for both the inhibitors; the results are shown in Table 5.

$$\Delta G_{ads.} = -RT \ln(55.5K) \qquad (6)$$

The negative sign of ΔG_{ads} indicates that the adsorption of the inhibitors on the steel surface is favorable from thermodynamics point of view. Hence the adsorption of the both inhibitors on mild steel surface in 1 M HCl solution is proceeding spontaneously. The values of ΔG_{ads} calculated by the three methods for the inhibitors are around −38 up to −35 kJ mol^{-1}. These values are at the interval of physical adsorption and chemical binding and indicate the chemical adsorption (chemisorption) of the inhibitors on the steel surface [23,24]. Chemisorptive bonds would normally be

Fig. 9 Arrhenius slopes calculated from corrosion current density for mild steel in 1 M HCl in the absence and presence of the inhibitors at 25°C

formed when Fe atoms on the metal surface share an election pair with the organic inhibitor reaction center. Considering the structure of Indigo dye and Nile Blue, with the possibility of high electron density around the oxygen and nitrogen atoms, the formation of Fe–O or even Fe–N bonds may be possible [13,19].

Effect of temperature

To find the activation energy of dissolution of mild steel, polarization measurements were performed at temperatures that range at 25–55°C in the absence and presence of the inhibitors, and the values of obtained polarization parameters (polarization curves are not show) are given in Table 6. Figure 9 shows the logarithm of corrosion currents against the reciprocal of the temperature. According to the Arrhenius equation, activation energy of metal dissolution in both media can be calculated from the slope of this curve as [20].

$$\ln I_{\mathrm{corr}} = \ln A - \frac{E_{\mathrm{a}}}{RT} \qquad (7)$$

The calculated activation energies in 1 M HCl with the absence and presence of Indigo Carmine and Nile Blue were 38.01, 71.95, and 44.93 kJ/mol, respectively.

It can be found that the energy barrier of corrosion reaction increases with the presence of the inhibitors; in the literature, the lower activation energy value of corrosion process in the presence of the inhibitor (rather than the absence of inhibitor) is attributed to its chemisorptions. In chemisorption or physical adsorption leading to the formation of an adsorptive film of electrostatic character, the temperature can modify the interaction between the steel electrode and the acidic media without and with the inhibitors [5,20,25]. The increased activation energies in the presence of the inhibitors may be attributed to the change in the mechanism of the corrosion process in the presence of adsorbed inhibitors molecules [5,20].

Conclusions

Indigo Carmine and Nile Blue are two organic dyes inhibitors for corrosion of mild steel in 1 M hydrochloric acid. The maximum inhibition efficiencies of Indigo Carmine were obtained in 9.65×10^{-05} M (%IE~98%). Inhibition efficiencies of Nile Blue increased with increasing in the inhibitor concentration up to 8.69×10^{-04} M (%IE~75–80%), but above this concentration, the solubility of Nile Blue decreases and it started to precipitate. The results obtained from weight loss, polarization, and EIS, for the both inhibitors, were in good agreement. Indigo Carmine and Nile Blue acted as a mixed-type inhibitor, and their inhibition mechanism obeys from the chemisorption interaction between the inhibitor and the mild steel. The calculated activation energies in 1 M HCl with the absence and presence of Indigo Carmine and Nile Blue were 38.01, 71.95, and 44.93 kJ/mol, respectively. Interpreting the values of the activation energies verified the chemisorption behavior of both inhibitors in the acidic media.

References

1. Abdel Rehim SS, Hazzazi OA, Amin MA, Khaled FK (2008) Corros Sci 50:2258
2. Machnikova E, Whitmire Kenton H, Hackerman N (2008) Electrochim Acta 53:6024
3. Noor Ehteram A, Al-Moubaraki AH (2008) Mater Chem Phys 110:145
4. Abboud Y, Abourriche A, Saffaj T, Berrada M, Charrouf M, Bennamara A, Cherqaoui A, Takky D (2006) Appl Surf Sci 252:8178
5. Ashassi-Sorkhabi H, Es'haghi M (2009) J Solid State Electrochem 13:1297–1301
6. Li X, Deng Sh FuH, Mu G (2009) Corros Sci 51:620
7. Lebrini M, Traisnel M, Lagrene´e M, Mernari B, Bentiss F (2008) Corros Sci 50:473
8. Quraishi MA, Shukla SK (2009) Mater Chem Phys 113:685
9. Ashassi-Sorkhabi H, Es'haghi M (2009) Mater Chem Phys 114:267
10. Oguzie EE, Njoku VO, Enenebeaku CK, Akalezi CO, Obi C (2008) Corros Sci 50:3480
11. Ashassi-Sorkhabi H, Seifzadeh D, Hosseini MG (2008) Corros Sci 50:3363
12. Ashassi-Sorkhabi H, Seifzadeh D (2008) J Appl Electrochem 38:1545
13. Abboud Y, Abourriche A, Saffaj T, Berradaa M, Charrouf M, Bennamara A, Hannache H (2009) Desalination 237:175
14. Ebensoa EE, Oguzie EE (2005) Mater Lett 59:2163
15. Oguzie EE (2005) Mater Lett 59:1076
16. Oguzie EE (2004) Mater Chem Phys 87:212
17. Ashassi-Sorkhabi H, Masoumi B, Ejbari P, Asghari E (2009) J Appl Electrochem 39:1497–1501
18. Ebenso EE, Alemu H, Umoren SA, Obot IB (2008) Int J Electrochem Sci 3:1325
19. Oguzie EE, Unaegbu C, Ogukwe CN, Okolue BN, Onuchukwu AI (2004) Mater Chem Phys 84:363
20. Avci G (2008) Colloids Surf A 317:730
21. Rammelt U, Koehler S, Reinhard G (2008) Corros Sci 50:1659
22. Abdeli M, Parvini-Ahmadi N, Khosroshahi RA (2009) Corrosion inhibition of mild steel in hydrochloric acid by 6-aminohexanoic acid. Mater Corros. doi:10.1002/maco.200905261
23. Zhao P, Zhong Ch, Hunag L, Niu L, Zhang F (2008) Corros Sci 50:2166
24. Hamdy HH (2007) Electrochim Acta 53:1722
25. Libin T, Xueming L, Lin L, Qing Q, Guannan M, Guangheng L (2005) Mater Chem Phys 94:353